Development 134, 261-272 (2007) doi:10.1242/dev.02721

Transcriptome and phenotypic analysis reveals Gata3-dependent signalling pathways in murine hair follicles

Dorota Kurek[1], George A. Garinis[2], J. Hikke van Doorninck[3], Jacqueline van der Wees[1] and Frank G. Grosveld[1,*]

The transcription factor Gata3 is crucially involved in epidermis and hair follicle differentiation. Yet, little is known about how Gata3 co-ordinates stem cell lineage determination in skin, what pathways are involved and how Gata3 differentially regulates distinct cell populations within the hair follicle. Here, we describe a conditional *Gata3*$^{-/-}$ mouse (K14-*Gata3*$^{-/-}$) in which *Gata3* is specifically deleted in epidermis and hair follicles. K14-*Gata3*$^{-/-}$ mice show aberrant postnatal growth and development, delayed hair growth and maintenance, abnormal hair follicle organization and irregular pigmentation. After the first hair cycle, the germinative layer surrounding the dermal papilla was not restored; instead, proliferation was pronounced in basal epidermal cells. Transcriptome analysis of laser-dissected K14-*Gata3*$^{-/-}$ hair follicles revealed mitosis, epithelial differentiation and the Notch, Wnt and BMP signaling pathways to be significantly overrepresented. Elucidation of these pathways at the RNA and protein levels and physiologic endpoints suggests that Gata3 integrates diverse signaling networks to regulate the balance between hair follicle and epidermal cell fates.

KEY WORDS: Gata3, Hair follicle, Epidermis, Laser capture microscopy, Microarray, Mouse

INTRODUCTION

The hair follicle (HF) comprises a discrete anatomical and physiological entity composed of epidermal stem cells that give rise to proteinaceous fibers (i.e. hair shafts) in response to growth factors (Schmidt-Ullrich and Paus, 2005). The HF is a mammalian organ that undergoes cyclic transformations, thereby allowing the study of fundamental developmental processes (e.g. proliferation, differentiation). The hair shaft and adjacent multi-layered inner root sheath (IRS) originate from the epithelial matrix that surrounds the dermal papilla, the permanent mesenchymal portion of the HF. In response to signals from the papilla, proliferating epithelial cells protrude into the dermis forming the first HF. Undifferentiated matrix cells remain in the hair bulb interacting with the dermal papilla (Cotsarelis et al., 1990; Oliver and Jahoda, 1988), or else differentiate as they migrate towards the epidermis.

An outer root sheath (ORS) surrounds the follicle that is contiguous with and biochemically similar to the basal epidermal layer. The bulge region is located beneath the sebaceous gland of the HF, marking the lowest point of the upper part of the follicle that is permanent. It contains a reservoir of stem cells able to repopulate HF lineages (Fuchs et al., 2004; Morris et al., 2004; Oshima et al., 2001; Taylor et al., 2000). HFs undergo self-renewal throughout life. Each hair cycle starts with a growth phase (anagen) where a germinative layer is formed around the dermal papilla derived from stem cells present in the bulge (Morris et al., 2004). Then, during catagen, the lower epithelial part regresses followed by resting and shedding periods (the telogen and exogen phases, respectively). Eventually, the lower part of the follicle grows downwards again to generate a new hair (Hardy, 1992).

[1]Department of Cell Biology, [2]Department of Genetics and [3]Department of Obstetrics and Gynecology, Erasmus Medical Center, P.O. Box 1738, 3000 DR Rotterdam, The Netherlands.

*Author for correspondence (e-mail: f.grosveld@erasmusmc.nl)

Accepted 31 October 2006

Gata3, a zinc finger transcription factor essential for the proper development of various tissues and organs (Pandolfi et al., 1995) is known to be involved in HF development and skin cell lineage determination (Ellis et al., 2001; Kaufman et al., 2003). Using skin transplantation experiments, Gata3 was shown to be crucially involved in skin cell lineage determination; its absence resulted in dysfunctional IRS precursor cells that could not differentiate properly (Kaufman et al., 2003). To examine how Gata3 exerts its role in IRS cell lineage determination and to identify potential Gata3 target genes, we generated K14-*Gata3*$^{-/-}$ mice to specifically ablate *Gata3* expression, thereby revealing its central role in mouse epidermis and HF development.

MATERIALS AND METHODS

Targeting and homologous recombination

The *Gata3* conditional knockout construct is shown in Fig. 1. E14 ES cells were electroporated, screened and germ line chimaeric mice generated by blastocyst injection. The PGKPuro cassette was removed by flp recombinase flpe6 (Buchholz et al., 1998).

Laser-capture microdissection and microarray analysis

Laser-capture microdissection was performed on 10 μm cryosections using the PALM MicroBeam microscope system (PALM Microlaser Technologies). RNA was analysed as described (http://www.affymetrix.com/index.affx). Microarray chips were analyzed with Affymetrix GeneChip software. Microarray data complied with the MIAME regulations and are available in ArrayExpress (accession code: 5988).

In situ hybridization, TUNEL and skin barrier

In situ hybridization with antisense digoxigenin-UTP-labelled RNA probes on 10 μm sections of skin samples was performed as described (Schaeren-Wiemers and Gerfin-Moser, 1993). Cell death was detected with the Cell Death Detection Kit, Fluorescein (Roche). Skin barrier experiments were performed as described (Hardman et al., 1998).

Immunohistochemistry, X-Gal staining and BrdU labelling

Mice were injected with 50 mg/kg bodyweight BrdU and sacrificed 2 hours later. Cryosections were fixed for 10 minutes in 4% PFA in PBS, then blocked with 1% BSA, 0.05% Tween in PBS. Primary antibodies were: K6 (rabbit, 1:5,000; Covance, PRB-169P), K14 (rabbit, 1:10,000; Covance, PRB-155P), Gata3 (mouse, 1:200; Santa Cruz, HCG3-31), CD3 (rat, 1:100; Santa Cruz, KT3), cyclin A2 (rabbit, 1:100; Santa Cruz, C-19), Cdk4 (rabbit, 1:100; Santa

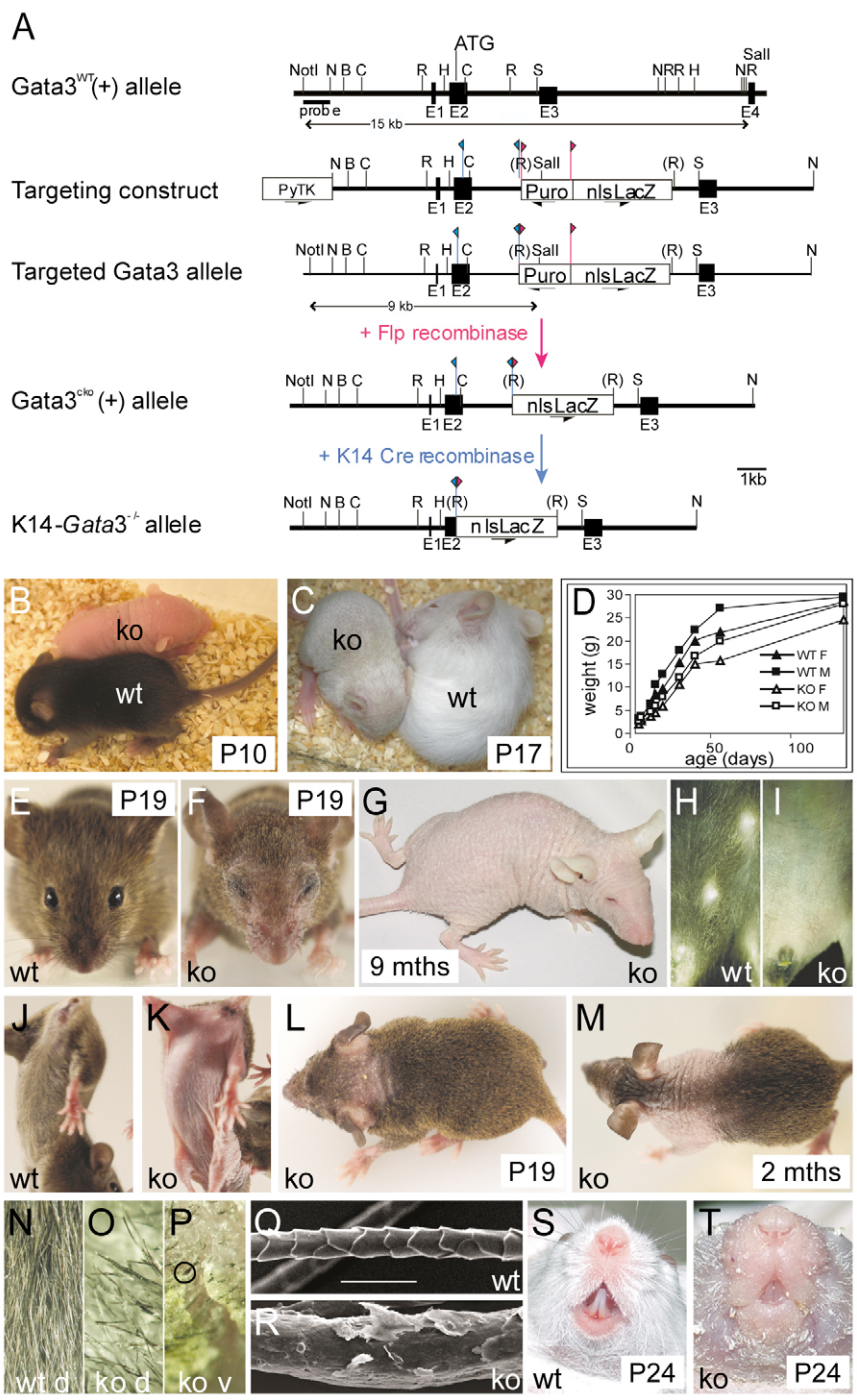

Fig. 1. (A) Generation of floxed/deleted *Gata3* alleles. LoxP sites were introduced in the start codon (in exon 2) and in the second intron (blue flags) of *Gata3*. A *Puro* cassette, flanked by FRT sites (pink flags) and coupled to an *nlsLacZ* gene lacking a polyA signal was introduced in intron 2. Arrows indicate lengths of *Not*I-*Sal*I restriction enzyme fragments that hybridize to the external 5′ probe. A Polyoma thymidine kinase gene (*PyTK*) was added 5′ to the construct to counter select against random integration. Flp recombinase mice (Buchholz et al., 1998) were used to remove the *Puro* cassette. After recombination by Cre recombinase, resulting in excision of the part of exon 2 that is 3′ to the start ATG of *Gata3* and the part of intron 2 that is 5′ to the *EcoR*I site, the *nlsLacZ* reporter replaces the 3′ end of the truncated *Gata3* gene. Arrows below genes indicate direction of transcription. Black boxes correspond to exons. B, *Bam*HI; C, *Cla*I; H, *Hin*dIII; N, *Nco*I; R, *Eco*RI; S, *Sac*I. (**B-T**). Phenotypes caused by homozygous deletion of *Gata3* in the skin (ko) versus wt. (B) Delayed hair growth in K14-*Gata3*$^{-/-}$ at P10. (C) Short stubby hairs instead of normal coat of fur. (D) Weight difference in the first months of life. (E,F) Eyes are still closed, whiskers are present but rudimentary, most facial hairs have disappeared and remaining hairs are still very short. (G) After 3 months, most K14-*Gata3*$^{-/-}$ mice are completely bald; eyes are still closed. (H,I) The absence of visible nipples in female K14-*Gata3*$^{-/-}$ mice. (J,K) The complete loss of hairs from the abdominal area at 2 months. (L,M) Baldness starts at the head and progress from anterior to posterior. (N-P) Coat of fur at P26. d, dorsal; v, ventral. (N) wt back hair; (O) K14-*Gata3*$^{-/-}$ back hair; (P) K14-*Gata3*$^{-/-}$ belly hair (and flakes; note the encircled, thick rounded tip of the hair instead of the normal fine hair tips). (Q,R) Scanning electron microscopy of dorsal wt (Q) and K14-*Gata3*$^{-/-}$ (R) hairs of 12-week-old mice. Note thickness of K14-*Gata3*$^{-/-}$ hair as well as absence of regular cuticle cells and presence of irregular flakes. (S,T) Around P24, K14-*Gata3*$^{-/-}$ skin starts flaking. Scale bar in Q: 50 μm for Q,R.

Cruz, C-22), cyclin E1 (rabbit, 1:100; Santa Cruz, M-20), loricrin (rabbit, 1:500; Covance, PRB 145P), K14 (rabbit, 1:10,000: Covance, PRB_155P), β-catenin (mouse, 1:100; BD, #14), AE13 (mouse, 1:20) (Lynch et al., 1986), AE15 (mouse, 1:10) (O'Guin et al., 1992), MTS24 (rat, 1:200) (Gill et al., 2002), BrdU (mouse, 1:100; DAKO, #Bu20a) and K10 (mouse, 1:50; Sigma, #k8.60). Relevant FITC-, TxR- or HRP-conjugated goat secondary antibodies (1:100, DAKO) were used. For BrdU immunohistochemistry, tissue was fixed in 4% PFA, 4°C overnight and subsequently embedded in paraffin and sectioned at 7 μm. After deparaffination, sections were boiled in 0.01 M citrate buffer (pH 6.0) for 15 minutes prior to primary antibody incubation. For X-Gal staining, sections were fixed for 1 minute in 0.5% glutaraldehyde, 1% PFA, and incubated in X-Gal staining solution for 5 hours at room temperature. Images were taken with an Olympus BX40 microscope and Axio Imager (Zeiss) fluorescence microscope.

RESULTS

Generation of keratinocyte-specific *Gata3*$^{-/-}$ mice (K14-*Gata3*$^{-/-}$)

The role of Gata3 in HF development was examined in mice expressing human keratin 14 promoter-driven Cre recombinase that restricts expression in the basal layer of stratified squamous epithelia and the ORS of HFs (Jonkers et al., 2001; Vassar et al., 1991). These mice were crossed with conditional *Gata3* knockout (*Gata3*cko) mice (Fig. 1A). The human K14 promoter drives *Cre* expression (visualized in a floxed Rosa-LacZ reporter mouse line) in epidermis, all HF cell types, salivary gland, mammary epithelium and epithelial cells from other tissues (Jonkers et al., 2001). We detected *Cre*

activity in the epidermis at embryonic day (E) 13.5, whereas placodes were *Cre*-positive two days before the onset of *Gata3* expression (i.e. E15.5). Heterozygous skin-specific *Gata3* knockouts were indistinguishable from wild-type (wt) littermates (not shown). K14cre/*Gata3*cko/wt mice were crossed with heterozygous and homozygous *Gata3*cko mice to generate K14cre/*Gata3*cko mice (referred to as K14-*Gata3*$^{-/-}$ or ko mice). These lacked expression of Gata3 in the hair follicles and epidermis at all stages, as determined by immunohistochemistry (not shown).

Aberrant postnatal growth and delayed development in K14-*Gata3*$^{-/-}$ mice

At birth, K14-*Gata3*$^{-/-}$ mice were morphologically and histologically indistinguishable from wt littermates, ruling out severe impaired embryonic development. However, from postnatal day (P) 2 onwards, K14-*Gata3*$^{-/-}$ mice demonstrated aberrant growth and delayed development resulting in dwarfism (Fig. 1B,C) and weight loss (Fig. 1D) during the first month of life. Further analysis revealed a half-opened-eye phenotype (Fig. 1E,F), stiff hind legs (Fig. 1G) and absence of visible nipples in K14-*Gata3*$^{-/-}$ mice (Fig. 1H,I). Importantly, K14-*Gata3*$^{-/-}$ hair development was delayed, hair growth was abnormal and replacement was sparse, if not absent, gradually resulting in bald mice (Fig. 1G).

Delayed hair growth and disturbed hair maintenance in K14-*Gata3*$^{-/-}$ mice

In contrast to wt, where external hairs were visible from P7, forming a well-developed fur coat by about P10, K14-*Gata3*$^{-/-}$ mice remained completely bald (Fig. 1B). From P12 onwards, hair growth was sparse around the head and neck resulting in a thin fur coat with short and stubby hairs (P17, Fig. 1C). The delayed onset of hair growth was followed by the gradual loss of abdominal hair (P19, Fig. 1J,K) and an anterior to posterior hair shedding in the head area (Fig. 1L,M), with limited hair regeneration. Remaining hairs appeared irregular, with a short, thick and hard appearance and a thick-rounded tip instead of the normally observed thin tip (Fig. 1N-R). Whiskers appeared short and thick (Fig. 1E,F,S,T).

Aberrant hair follicle organization and abnormal hair pigmentation in K14-*Gata3*$^{-/-}$ mice

At P0, K14-*Gata3*$^{-/-}$ HFs appeared normal. However, beginning at P3, K14-*Gata3*$^{-/-}$ HFs were abnormal and grew at a much wider angle, often parallel to the skin surface, never reaching the epidermis (Fig. 2H). However, the overall number of HFs was not reduced, suggesting that Gata3 is not essential during HF induction. Whereas wt hairs had the typical ladder-like appearance resulting from the large, keratinized pigment-containing cells interspersed with air pockets in the hair medulla, the K14-*Gata3*$^{-/-}$ hair pigment deposition was disorganized and without air spaces (Fig. 1R, Fig. 2F) and the sebaceous glands were enlarged from P7 onwards. Subsequently, the K14-*Gata3*$^{-/-}$ HF entered telogen after a delayed catagen lasting at least 6 days instead of the normal 3 days (see Fig. S1A-F in the supplementary material) and the HF proximal end failed to reform (see Fig. S1I,J in the supplementary material). New visible hairs were not produced, although some developing HFs and small cysts were visible (see Fig. S1J in the supplementary material).

The newly formed HFs that derive from stem cells (Morris et al., 2004) are known to migrate from the bulge to the matrix area of the hair bulb, thereby forming a germinative layer that becomes committed to distinct HF cell lineages (Legue and Nicolas, 2005). The lack of HF renewal prompted us to investigate whether Gata3 is

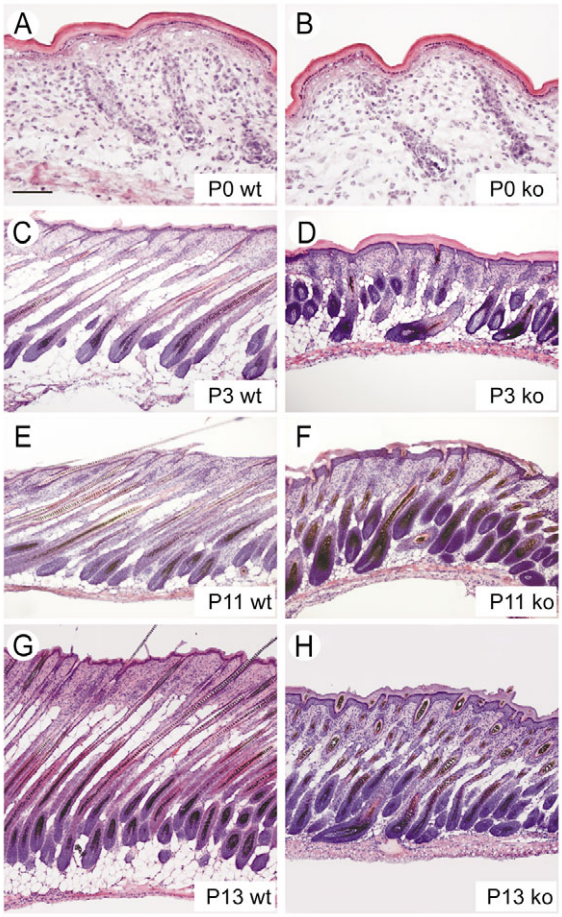

Fig. 2. Haematoxylin-Eosin staining of fresh-frozen dorsal skin sections of control and K14-*Gata3*$^{-/-}$ mice. (**A**,**B**) P0: skin of K14-*Gata3*$^{-/-}$ is indiscernible from control skin. (**C**,**D**) P7: in K14-*Gata3*$^{-/-}$ HFs are disorganized and do not produce hairs. Epidermis is thickened. (**E**,**F**) P11: in the mutant, (abnormal) hairs are still not penetrating the epidermis. (**G**,**H**) P13: some irregularly formed hairs penetrate the skin; both dermis and subcutaneous fat layer (white cells) are much thinner in K14-*Gata3*$^{-/-}$ than in control skin. Scale bar in A: 50 μm for A,B; 200 μm for C-H.

also expressed in cells other than those of the IRS (Kaufman et al., 2003). Evaluation of Gata3 expression in Gata3 LacZ knock-in mice and by in situ hybridization revealed Gata3 to be readily expressed in other skin structures (Pata et al., 1999) (Fig. 3 and see Fig. S2 in the supplementary material). At E15.5, *Gata3* was expressed in the epidermis (Fig. 3A), whereas during anagen *Gata3* was also expressed in the IRS, ORS, sebaceous glands, epidermis and infundibulum (Fig. 3B-L, and see Fig. S2 in the supplementary material) and in certain germinative layer cells surrounding the dermal papilla (Fig. 3F,J,L). During catagen, *Gata3* expression was restricted to the IRS (Fig. 3G), whereas during telogen it was present in the epidermis and sebaceous glands, butabsent from the HF (Fig. 3H).

Epidermal hyperplasia and hyperkeratosis in K14-*Gata3*$^{-/-}$ skin

Instead of developing new HF bulbs, we noticed pronounced hyperplasia in the *K14*-Gata3$^{-/-}$ epidermis (see below). Despite a slightly delayed barrier function in fetuses at E16.5, E17.5 and E18.5 (data not shown), initial development of the epidermis appeared

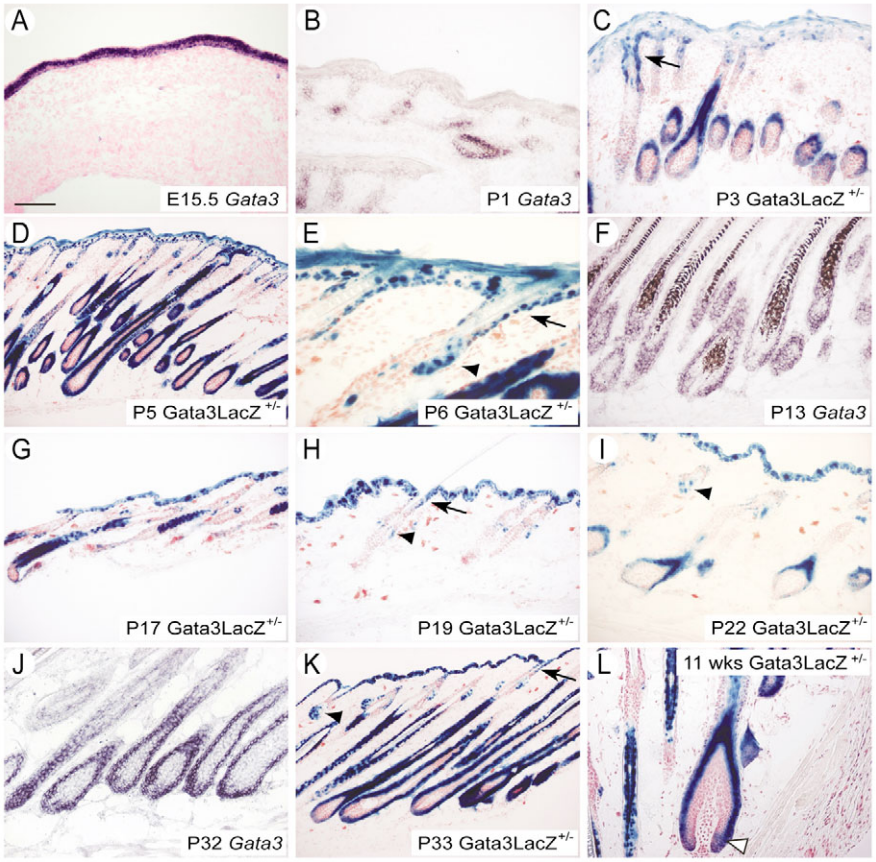

Fig. 3. Expression pattern of *Gata3* during the cell cycle. Gata3 expression is visualized by in situ hybridization in the control (**A**,**B**,**F**,**J**), or by X-Gal staining in the *Gata3* LacZ knockin skin (**C-E**,**G-I**,**K**,**L**). At E15.5 there is strong expression of *Gata3* in the epidermis (A). During anagen (A, P3), Gata3 is highly expressed in the IRS, ORS, sebaceous glands (black arrowhead), epidermis and infundibulum (arrows) (B-F,I-L,), and closer inspection (L) reveals that some cells in the germinative layer around the dermal papilla are also *Gata3* positive (white arrowhead). During catagen, *Gata3* expression was restricted to the IRS (G) and was absent in HF during telogen but present in the epidermis and sebaceous gland (H). Scale bar in A: 200 μm for D,K; 150 μm for A-C,F,G-J,L; 50 μm for E.

normal in skin sections from newborn mice (P0, Fig. 2A,B and P3, Fig. 2C,D). At P3, skin hyperplasia was followed by wrinkles (Fig. 2E-H) covered with squames (Fig. 1T). K14-*Gata3*$^{-/-}$ skin sections, at different ages, revealed gradual, pronounced epidermal thickening including that of basal and suprabasal layers (see Fig. S3B,D in the supplementary material) as well as the development of hyperkeratosis (increased thickness of stratum corneum; Fig. 2C-H and see Fig. S3B,C in the supplementary material). We did not observe any nuclei in the squames of stratum corneum that would mark the presence of immaturely shed keratinocytes, a feature that is routinely observed in psoriasis. In contrast to the thickened epidermis, the dermis of K14-*Gata3*$^{-/-}$ pups appeared substantially thinner, along with a reduction in subcutaneous adipose tissue as compared with wt littermates (Fig. 2G,H).

Transcriptome analysis in K14-*Gata3*$^{-/-}$ HF

To obtain unbiased insight into the HF phenotype of K14-*Gata3*$^{-/-}$ mice, we implemented a laser-capture approach (Fig. 4A-F) to isolate the proximal end of HFs from 11-day-old wt and K14-*Gata3*$^{-/-}$ mouse skin (by then, the K14-*Gata3*$^{-/-}$ skin phenotype is fully developed, n=6, Fig. 4G,H) and examined their transcriptome profiles. Two-tail, pair-wise analysis of variance revealed 1516 genes with significantly different expression patterns between the two genotypes (P<0.01, >1.2-fold up- or downregulated; Fig. 4H and see Table S1 in the supplementary material). This substantially exceeds the ~80 genes expected to occur by chance under these selection criteria.

To avoid any preselection of genes and thus the potential introduction of bias, we used a previously described methodology (Hosack et al., 2003) to identify all over-represented biological processes in our dataset [i.e. cell cycle, epithelial growth and differentiation, immune and defense responses, signal transduction pathways and energy metabolism (Fig. 4G)]. Analysis of these processes (Fig. 4H, and see Table S1 in the supplementary material) led us to identify:

(1) The downregulation of genes associated with the mitotic cell cycle and replication, and the upregulation of genes associated with nucleosomal assembly, suggesting that cells in the K14-*Gata3*$^{-/-}$ HF require Gata3 to progress successfully through the cell cycle.

(2) The downregulation of pro-apoptotic genes and the upregulation of anti-apoptotic genes. This supports the notion that proliferation, differentiation and apoptosis are co-regulated processes all requiring Gata3 constitutive levels in the developing HF; the dampening of apoptosis paralleled the inability of K14-*Gata3*$^{-/-}$ HF cells to progress through the cell cycle.

(3) The upregulation of genes associated with epithelial growth and differentiation (e.g. several keratin and keratin-associated genes). This is likely to reflect the presence of incompletely differentiated cell types.

(4) The suppression of all genes associated with immune, inflammatory and defense responses and the downregulation of genes associated with fatty acid synthesis and storage, confirming the considerable loss of fat in the dermis of K14-*Gata3*$^{-/-}$ mice (Fig. 2H).

(5) The up- or downregulation of genes associated with the FGF, Notch, Wnt and BMP signaling pathways.

PCR evaluation of the expression levels of several genes in the HF of K14-*Gata3*$^{-/-}$ mice and wt littermates confirmed the validity of the microarray data (see Fig. S7 in the supplementary material).

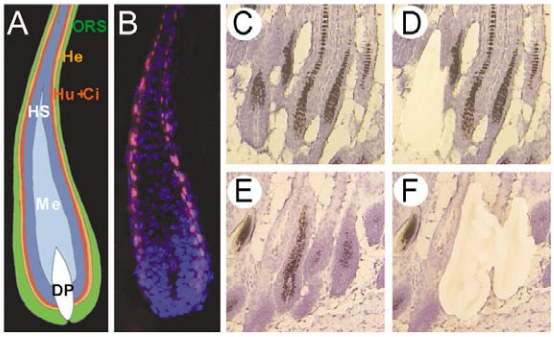

G

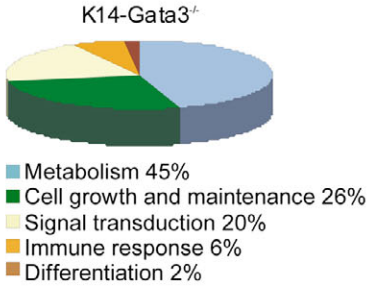

H

Code	Gene description	Symbol	FC	P
Cell cycle				
1417911_at	cyclin A2	Ccna2	-1.94	0.0000
1448205_at	cyclin B1	Ccnb1	-1.87	0.0000
1422513_at	cyclin F	Ccnf	-2.32	0.0005
1420827_a_at	cyclin G1	Ccng1	-1.38	0.0016
1416488_at	cyclin G2	Ccng2	-1.53	0.0034
1417131_at	cell division cycle 25 homolog A	Cdc25a	-1.60	0.0105
1421963_a_at	cell division cycle 25 homolog B	Cdc25b	-1.33	0.0042
1456077_x_at	cell division cycle 25 homolog C	Cdc25c	-1.69	0.0051
1448314_at	cell division cycle 2 homolog A	Cdc2a	-1.63	0.0002
1422016_a_at	centromere autoantigen H	Cenph	-1.58	0.0073
1439436_x_at	inner centromere protein	Incenp	-1.71	0.0009
1417299_at	NIMA -related expressed kinase 2	Nek2	-2.63	0.0000
1419620_at	pituitary tumor-transforming 1	Pttg1	-2.32	0.0009
1416161_at	RAD21 homolog (S. pombe)	Rad21	-1.42	0.0039
1417830_at	struct.maint.of chromosomes 1-l1	Smc1l1	-1.29	0.0003
1458479_at	struct.maint. of chromosomes 2-l1	Smc2l1	-1.89	0.0109
1427275_at	struct.maint. of chromosomes 4-l1	Smc4l1	-1.80	0.0037
1452954_at	ubiquitin-conjugating enzyme E2C	Ube2c	-1.85	0.0000
1424046_at	budding uninh/ed by benz/oles 1	Bub1	-1.68	0.0015
1447363_s_at	budding uninh/ed by benz/oles 1b	Bub1b	-1.90	0.0000
Epidermal differentiation				
1421589_at	keratin complex 1, acidic, gene 1	Krt1-1	3.41	0.0006
1460347_at	keratin complex 1, acidic, gene 14	Krt1-14	1.76	0.0036
1422667_at	keratin complex 1, acidic, gene 15	Krt1-15	2.91	0.0000
1448932_at	keratin complex 1, acidic, gene 16	Krt1-16	11.28	0.0000
1423227_at	keratin complex 1, acidic, gene 17	Krt1-17	2.27	0.0001
1417156_at	keratin complex 1, acidic, gene 19	Krt1-19	1.65	0.0034
1420409_at	keratin complex 1, acidic, gene 24	Krt1-24	1.40	0.0007
1427179_at	keratin complex 1, acidic, gene 3	Krt1-3	6.15	0.0002
1418742_at	keratin complex 1, acidic, gene 4	Krt1-4	9.30	0.0007
1427751_a_at	keratin complex 1, acidic, gene 5	Krt1-5	6.25	0.0000
1427365_at	keratin complex 2, basic, gene 10	Krt2-10	7.50	0.0000
1460185_at	keratin complex 2, basic, gene 18	Krt2-18	2.29	0.0001
1427290_at	keratin complex 2, basic, gene 19	Krt2-19	6.39	0.0003
1424096_at	keratin complex 2, basic, gene 5	Krt2-5	1.21	0.0022
1422784_at	keratin complex 2, basic, gene 6a	Krt2-6a	4.36	0.0000
1450536_s_at	keratin associated protein 12-1	Krtap12-1	8.70	0.0000
1419707_at	keratin associated protein 14	Krtap14	4.21	0.0015
1419507_at	keratin associated protein 15	Krtap15	5.10	0.0004
1425655_at	keratin associated protein 16-1	Krtap16-1	25.58	0.0000
1427549_s_at	keratin associated protein 16-10	Krtap16-10	6.40	0.0000
1427801_at	keratin associated protein 16-2	Krtap16-2	26.15	0.0000
1425431_at	keratin associated protein 16-3	Krtap16-3	10.22	0.0004
1426203_at	keratin associated protein 16-4	Krtap16-4	30.75	0.0000
1425430_at	keratin associated protein 16-5	Krtap16-5	32.73	0.0004
1425237_at	keratin associated protein 16-8	Krtap16-8	8.41	0.0000
1427366_at	keratin associated protein 3-1	Krtap3-1	8.09	0.0007
1452957_at	keratin associated protein 3-3	Krtap3-3	8.72	0.0005
1451859_at	keratin associated protein 6-1	Krtap6-1	8.31	0.0000
1449919_at	keratin associated protein 6-2	Krtap6-2	19.43	0.0000
1427842_at	keratin associated protein 6-3	Krtap6-3	5.22	0.0005
1427211_at	keratin associated protein 8-1	Krtap8-1	2.17	0.0006
1421689_at	keratin associated protein 8-2	Krtap8-2	14.74	0.0000
1441956_s_at	cut-like 1 (Drosophila)	Cutl1	-4.25	0.0012
Nucleosome assembly				
1455712_at	histone 3, H2bb	Hist3h2bb	5.84	0.0000
1416101_a_at	histone 1, H1c	Hist1h1c	5.06	0.0000
1430357_at	H3 histone, family 3B	H3f3b	4.32	0.0001
1425398_at	histone 1, H2bc	Hist1h2bc	4.21	0.0000
1449482_at	histone 3, H2ba	Hist3h2ba	3.10	0.0017
1435865_at	histone 3, H2a	Hist3h2a	2.89	0.0000
1418367_x_at	histone 2, H2aa1	Hist2h2aa1	2.86	0.0008
1442051_at	histone 2, H3c1	Hist2h3c1	2.61	0.0000
1455725_a_at	H3 histone 3B	H3f3b	1.24	0.0001

Code	Gene description	Symbol	FC	P
Immune and defense responses				
1455082_at	Casitas B-lineage lymphoma b	Cblb	-1.66	0.0022
1448569_at	CD8 antigen, beta chain	Cd8b	-1.51	0.0002
1418392_a_at	guanylate nucleotide binding protein 3	Gbp3	-3.42	0.0036
1449875_s_at	histocompatibility 2, T region locus 10	H2-T10	-2.51	0.0000
1449556_at	histocompatibility 2, T region locus 23	H2-T23	-4.37	0.0009
1452231_x_at	interf. activated gene 205	Ifi205	-2.89	0.0092
1450783_at	interf.-induced protein 1	Ifit1	-2.33	0.0012
1449025_at	interf.-induced protein 3	Ifit3	-5.13	0.0000
1448436_a_at	interf. regulatory factor 1	Irf1	-1.86	0.0057
1421322_a_at	interf. depend.(+) acting tr.factor 3g	Isgf3g	-2.87	0.0000
1424775_at	2'-5' oligoadenylate synthetase 1G	Oas1g	-15.19	0.0000
1453196_a_at	2'-5' oligoadenylate synthetase-like 2	Oasl2	-2.64	0.0002
1418131_at	SAM domain and HD domain, 1	Samhd1	-1.34	0.0023
1419307_at	tumor necrosis factor rec. 13c	Tnfrsf13c	-2.42	0.0001
Wnt signalling pathway				
1435373_at	casein kinase 1, epsilon	Csnk1e	1.73	0.0000
1417419_at	cyclin D1	Ccnd1	1.66	0.0006
1416123_at	cyclin D2	Ccnd2	-2.27	0.0003
1422985_at	frizzled homolog 1 (Drosophila)	Fzd1	2.94	0.0000
1450135_at	frizzled homolog 3 (Drosophila)	Fzd3	2.84	0.0000
1448662_at	frizzled homolog 6 (Drosophila)	Fzd6	1.69	0.0019
1416658_at	frizzled-related protein	Frzb	-1.54	0.0072
1449058_at	GLI-Kruppel family member GLI	Gli	-1.57	0.0005
1455277_at	Hedgehog-interacting protein	Hhip	-1.66	0.0002
1431947_at	low density lipoprotein receptor	Ldlr	-1.79	0.0017
1418634_at	Notch gene homolog 1 (Drosophila)	Notch1	1.71	0.0000
1417985_at	Notch-regulated ankyrin repeat protein	Nrarp	-2.40	0.0001
1422655_at	patched homolog 2	Ptch2	-2.84	0.0091
1418085_at	protein kinase C, zeta	Prkcz	2.12	0.0008
1451358_a_at	Rac GTPase-activating protein 1	Racgap1	-1.60	0.0000
1436869_at	sonic hedgehog	Shh	-2.37	0.0000
1426091_a_at	wingless-related MMTV integr.site 10b	Wnt10b	1.90	0.0024
1450772_at	wingless-related MMTV integr. site 11	Wnt11	3.58	0.0000
1450763_x_at	wingless-related MMTV integr. site 3	Wnt3	1.94	0.0006
1437673_at	wingless-related MMTV integr. site 5A	Wnt5a	-4.43	0.0001
1419708_at	wingless-related MMTV integr. site 6	Wnt6	-1.51	0.0053
1420006_at	bone morphogenetic protein 15	Bmp15	1.71	0.0025
1450759_at	bone morphogenetic protein 6	Bmp6	2.95	0.0000
1449873_at	bone morphogenetic protein 8a	Bmp8a	1.94	0.0002
Pro-apoptotic				
1425918_at	EGL nine homolog 3 (C. elegans)	Egln3	-3.55	0.0015
1422470_at	BCL2/adenovirus E1B inter. protein 1	Bnip3	-2.01	0.0047
1418901_at	CCAAT/enhancer binding protein beta	Cebpb	-1.80	0.0035
1437182_at	death inducer-obliterator 1	Dido1	-1.74	0.0050
1448449_at	receptor-interacting ser.-thr.kinase 3	Ripk3	-1.59	0.0080
1437503_a_at	scotin gene	Scotin-pendin	-1.49	0.0002
1451233_at	Tnf receptor-associated factor 2	Traf2	-1.47	0.0030
1449839_at	caspase 3	Casp3	-1.30	0.0088
1433699_at	TNF, alpha-induced protein 3	Tnfaip3	-1.25	0.0030
1435834_at	growth arrest specific 2	Gas2	-1.24	0.0048
1448809_at	chromosome segregation 1-like	Cse1l	-1.22	0.0079
Anti-apoptosis				
1434229_a_at	polymerase (DNA directed), beta	Polb	1.71	0.0001
1427127_x_at	heat shock protein 1B	Hspa1b	1.56	0.0008
1425281_a_at	glucocorticoid-induced leucine zipper	Gilz	1.78	0.0002
1454860_x_at	defender against cell death 1	Dad1	1.49	0.0084
1422452_at	Bcl2-associated athanogene 3	Bag3	1.89	0.0007

Fig. 4. Transcriptome analysis in K14-*Gata3*$^{-/-}$ HF. (**A-F**) Schematic of HF (A) and Gata3 expression in innermost layers of IRS at P11 (B). Fresh-frozen skin sections of P11 wt (C,D) and K14-*Gata3*$^{-/-}$ (E,F) before (C,E) and after (D,F) collecting HF tissue by laser-capture. RNA from the captured tissue was used for microarray analysis. DP, dermal papilla; He, Henle's layer of IRS; HS, hair shaft; Hu+Ci, Huxley's layer and cuticle of IRS; Me, medulla; ORS, outer root sheath. (**G**,**H**) Full mouse genome transcriptome analysis of laser-captured, K14-*Gata3*$^{-/-}$ and wt HFs. (G) Pie chart of significantly over-represented biological processes in K14-*Gata3*$^{-/-}$ as compared with wt HFs. (H) Significant gene expression changes in the K14-*Gata3*$^{-/-}$ as compared with wt mouse HFs (for an extensive overview, see Table S1 in the supplementary material). FC, fold change; P=*P*-value for two-tail analysis of variance.

Aberrant proliferation and cell cycle regulation in the K14-*Gata3*$^{-/-}$ hair follicle

The suppression of genes associated with the cell cycle machinery prompted us to evaluate the proliferative capacity and apoptosis in the HF. We found a significantly higher frequency of BrdU(+) cells in the K14-*Gata3*$^{-/-}$ basal epidermal layer at P7 (Fig. 5A-C) and P11-15 (data not shown). Subsequent analysis revealed a substantially higher frequency of BrdU(+) cells in the ORS that was continuous with the epidermis (Fig. 5D-F, area 'b'). In contrast to the wt HF, those cells located close to the hair bulb (i.e. hair matrix cells) most responsible for the nourishment of the growing hair (Fig. 5D-F, area 'a') demonstrated decreased BrdU incorporation. TUNEL (Fig. 5G-I) and caspase 3 (not shown) staining revealed reduced apoptosis in the K14-*Gata3*$^{-/-}$ skin, thereby confirming the previously observed suppression of pro-apoptotic genes, and suggesting that aberrant cell proliferation is likely to contribute to diminished hair growth. Furthermore, K14-*Gata3*$^{-/-}$ skin demonstrated an as yet unexplained reduction in T-cells (CD3) (Fig. 5J-L) and MHC class II cells (not shown), supporting the notion that the epidermal abnormalities are a direct consequence of *Gata3* loss in the mouse skin and are not secondary to inflammation (Fig. 5G,H).

The proliferative capacity of those cells located close to the hair bulb (Fig. 5E, area 'a'), as opposed to those located in the epithelial lining (area 'b'), in the K14-*Gata3*$^{-/-}$ HFs is in agreement with the aberrant regulation of genes associated with the cell cycle (Fig. 4H). In situ mRNA or protein expression analyses further confirmed the diminished cyclin D2, cyclin E1, cyclin A2 and Cdk4 in most cells located within the hair bulb as opposed to those lying along the HF ORS, as well as increased cyclin D1 expression in the ORS (see Fig. S4 in the supplementary material).

Keratins and keratin-associated proteins in K14-*Gata3*$^{-/-}$ mouse skin

Of the 34 keratin and keratin-associated proteins whose expression was significantly altered, 30 were overexpressed in K14-*Gata3*$^{-/-}$ mice. In particular, we noticed the increased expression of the Krtap16 gene family, ranging from ~6- to 33-fold, which was further

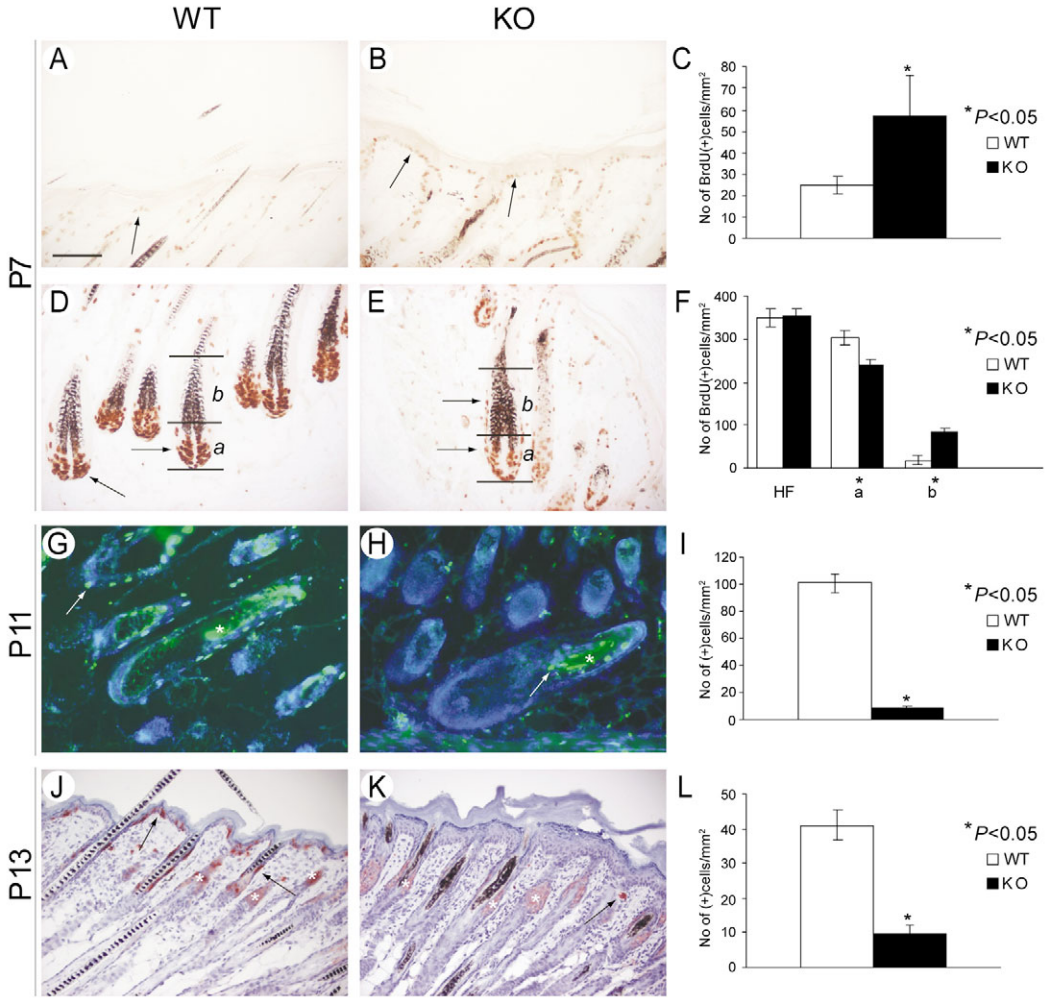

Fig. 5. Altered distribution of dividing cells, T-cell number and apoptosis in K14-*Gata3*$^{-/-}$ skin. (**A-F**) BrdU labeling of dividing cells of wt (left) and K14-*Gata3*$^{-/-}$ (right) skin. In wt animals, BrdU labeling (brown-stained nuclei) is mostly present in the bulb of the HFs (D). The cells of the basal layer of the K14-*Gata3*$^{-/-}$ epidermis are dividing at a much higher rate (compare A with B). There is no obvious difference in the number of BrdU-labelled HF cells, but in their distribution (compare regions a and b in D-F). (**G-I**) TUNEL assay shows altered apoptosis in K14-*Gata3*$^{-/-}$ skin as compared with control skin at P11. Arrows indicate positive cells (**J-L**): K14-*Gata3*$^{-/-}$ skin contains less CD3 positive T-cells (red dots, arrows) than wt skin. White asterisks mark background staining of an artifact of the knots of highly keratinized material (G,H) and sebaceous glands (J,K). Data are given as mean±s.e.m.; *, $P \leq 0.05$; Student's *t*-test. Scale bar in A: 150 μm for A,B,D,E,J,K; 100 μm for G,H.

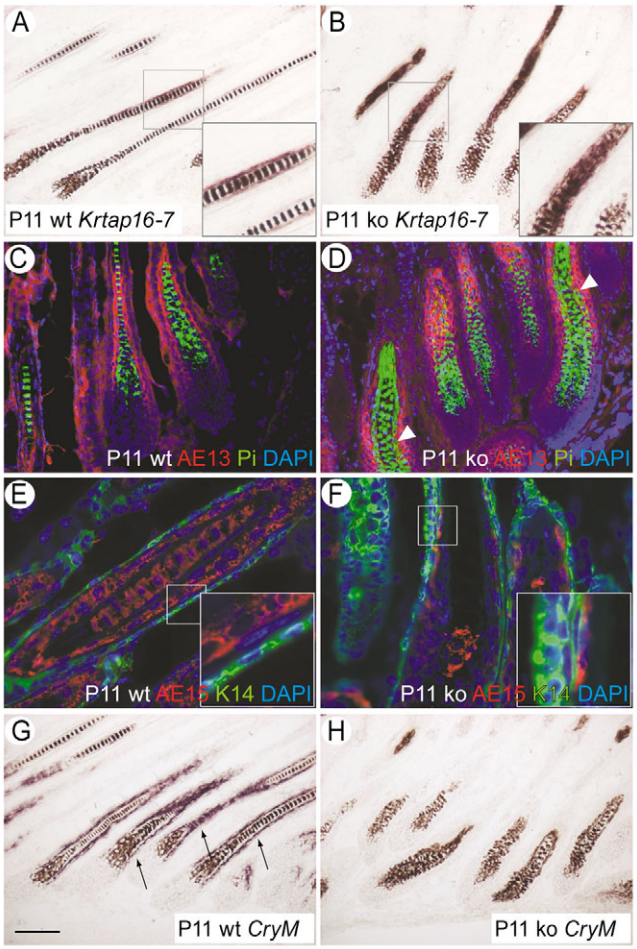

Fig. 6. Hair follicle in the absence of Gata3. (**A**,**B**) In situ mRNA hybridization of *Krtap16-7* at P11; insets show normal cortex expression in the wt (A), whereas expression spreads into the medulla in K14-*Gata3*$^{-/-}$ hairs (B). (**C**,**D**) Cortical cells recognized by AE13 antibody were no longer separate from the pigmented cells in K14-*Gata3*$^{-/-}$ HFs and those HFs exhibited expanded precortex and cortex as compared with wt HFs. Arrowheads indicate lack of separation of cortical cells from the pigmented cells. DAPI was used to mark the nuclei. (**E**,**F**) AE15 antibody recognizes trychohyalin IRS and medulla of control HFs (E) and only wisps of cells in K14-*Gata3*$^{-/-}$ IRS (F). There is a lack of separation of AE15-positive cells from K14-positive cells in K14-*Gata3*$^{-/-}$ HFs as compared with control (E,F, insets). (**G**,**H**) Expression of *Crym* at P11 in control (G) and K14-*Gata3*$^{-/-}$ skin (H); arrows in G point to expression in IRS. Scale bar in G: 200 μm for A,B,G,H; 100 μm for C,D; 50 μm for E,F.

confirmed by in situ mRNA evaluation of *Krtap16-7* (Fig. 6A,B). Its expression domain was not separate from the pigmented cells, suggesting that the cortex and medulla are no longer separated (Fig. 6A,B). Consistent with previous findings, AE13 antibody detected the acidic hair keratins expressed in the cortex and cuticle of the hair shaft (Lynch et al., 1986) (Fig. 6C), whereas K14-*Gata3*$^{-/-}$ HFs exhibited expanded precortex and cortex when compared with wt HFs (Kaufman et al., 2003) (Fig. 6D). Similar to *Krtap16-7*, the expression domain detected with the AE13 antibody was not separate from the pigmented cells (Fig. 6D, arrowheads).

AE15, an antibody that recognizes trychohyalin found in characteristic granules of the IRS and medulla (O'Guin et al., 1992) (Fig. 6E), detected a thin bundle of AE15(+) K14-*Gata3*$^{-/-}$ IRS cells (Kaufman et al., 2003) (Fig. 6F). Double staining with AE15 and K14 antibodies revealed that the companion layer did not separate AE15(+) and K14(+) cells (Fig. 6E,F).

Consistent with the absence of Huxley's layer and the cuticle of the IRS in K14-*Gata3*$^{-/-}$ HFs, expression of μ-crystallin (*Crym* – Mouse Genome Informatics), known to co-localize with Gata3 in the IRS (Fig. 6G) (Aoki et al., 2000), was diminished in K14-*Gata3*$^{-/-}$ HFs (Fig. 4H and Fig. 6H).

Next, we examined the differentiation status of K14-*Gata3*$^{-/-}$ mouse skin. Staining of loricrin, a late-stage differentiation marker, showed no differences in both young (P1, Fig. 7A,B) and mature (5 months, Fig. 7C,D) skin. In P4 skin, K10 expression was not different between the wt and K14-*Gata3*$^{-/-}$ mice (Fig. 7E,F). In P26, K10 was expressed in a layer surrounding the proximal part of K14-*Gata3*$^{-/-}$ HF, the ORS and the basal epidermal keratinocytes (Fig. 7H). In wt skin, however, it was restricted to suprabasal epidermal keratinocytes and infundibulum (Fig. 7G). K6, a cytokeratin known to mark proliferating cells proximal to the bulge and K10, was observed distal to the bulge and in the basal epidermis (Fig. 7I-K). Occasionally, K10 and K6 colocalized (Fig. 7K). At later stages, the number of K6-expressing cells in the skin increased substantially (Fig. 7L,M). Immunohistochemical analysis of K14, typically expressed in the ORS and the basal layer of stratified squamous epithelia of normal HFs (Vassar et al., 1989), confirmed our findings (Fig. 4H). Interestingly, the basal epidermal layer and ORS were almost twice as thick in K14-*Gata3*$^{-/-}$ compared with wt skin (Fig. 6E,F). Together, these changes indicate aberrant differentiation, which is likely to be due to the deregulation of signal transduction pathways.

Signal transduction and embryonic development in K14-*Gata3*$^{-/-}$ HFs

Most of the prominent signal transduction pathways known to be involved in HF morphogenesis were significantly over-represented in the K14-*Gata3*$^{-/-}$ HF transcriptome, including the Wnt and BMP families, sonic hedgehog and Notch (Fig. 4G-H). *Wnt3*, *Wnt10b*, and *Wnt11* were upregulated in K14-*Gata3*$^{-/-}$ HFs, whereas *Wnt5a* and *Wnt6* were downregulated compared with controls (Fig. 4H). In the wt HF, *Wnt5a* expression was detected in the ORS, IRS and dermal papilla (Fig. 8A), but was almost undetectable in K14-*Gata3*$^{-/-}$ HFs (Fig. 4H and Fig. 8B), a finding in agreement with the absence of differentiated IRS cells, the significant decrease in *Shh* mRNA levels (see below) and the known absence of *Wnt5a* expression in *Shh*$^{-/-}$ mice (Reddy et al., 2001). *Wnt11* was previously shown to be expressed in the outermost layers of the HF, ORS and dermal sheath, above the dermal papilla (Reddy et al., 2001) (Fig. 8C). Similar to K10 (Fig. 7H), *Wnt11* expression was expanded to the lowest (most proximal) part of the bulb in K14-*Gata3*$^{-/-}$ HFs (Fig. 8D), and was also present in the K14-*Gata3*$^{-/-}$ outer HF layer, as compared with controls. This could originate from an increased number of precursor IRS cells in the matrix that are in turn likely to be due to a migration defect that could also underlie the observed thickening of the matrix. Frizzled Wnt receptors *Fzd1*, *Fzd3* and *Fzd6* were overexpressed in the K14-*Gata3*$^{-/-}$ HF, whereas frizzled-related protein (*Frzb*, an inhibitor of Wnt signaling) was significantly downregulated (Fig. 4H). In agreement, we detected strong nuclear β-catenin staining in K14-*Gata3*$^{-/-}$ HFs (Fig. 8E,F). *Shh* along with *Gli1*, which is a known target and transducer of Shh signaling, the hedgehog-interacting protein (*Hhip*) and patched homolog 2 (*Ptch2*) demonstrated reduced expression levels in K14-*Gata3*$^{-/-}$ HFs (Fig. 4H). The decrease in *Gli1* expression levels was also confirmed by in situ hybridization in P7 K14-*Gata3*$^{-/-}$ HFs (Fig. 8G,H), particularly in the region of the dermal papilla.

Whereas *Notch1* was upregulated in the K14-*Gata3*$^{-/-}$ HF (Fig. 4H), the expression levels of *Notch2* and *Notch3* were not significantly affected. In situ mRNA hybridization showed *Notch1* to be expressed in precursor cells of cortex, cuticle, and IRS (Fig. 8I) (Kopan and Weintraub, 1993). Although the expression pattern of *Notch1* appeared unchanged in the K14-*Gata3*$^{-/-}$ HF, its expression levels were substantially higher, particularly in the lower matrix cells (Fig. 8J). Taken together, these findings support the notion that Gata3 plays a central role in Shh and Notch signaling pathways, though this effect is likely to be indirect as *Shh* and *Notch* are expressed in different cells.

Three BMP genes (*Bmp6*, *Bmp8a* and *Bmp15*) were overexpressed in K14-*Gata3*$^{-/-}$ HFs as compared with wt controls; by contrast, BMP-receptor expression did not

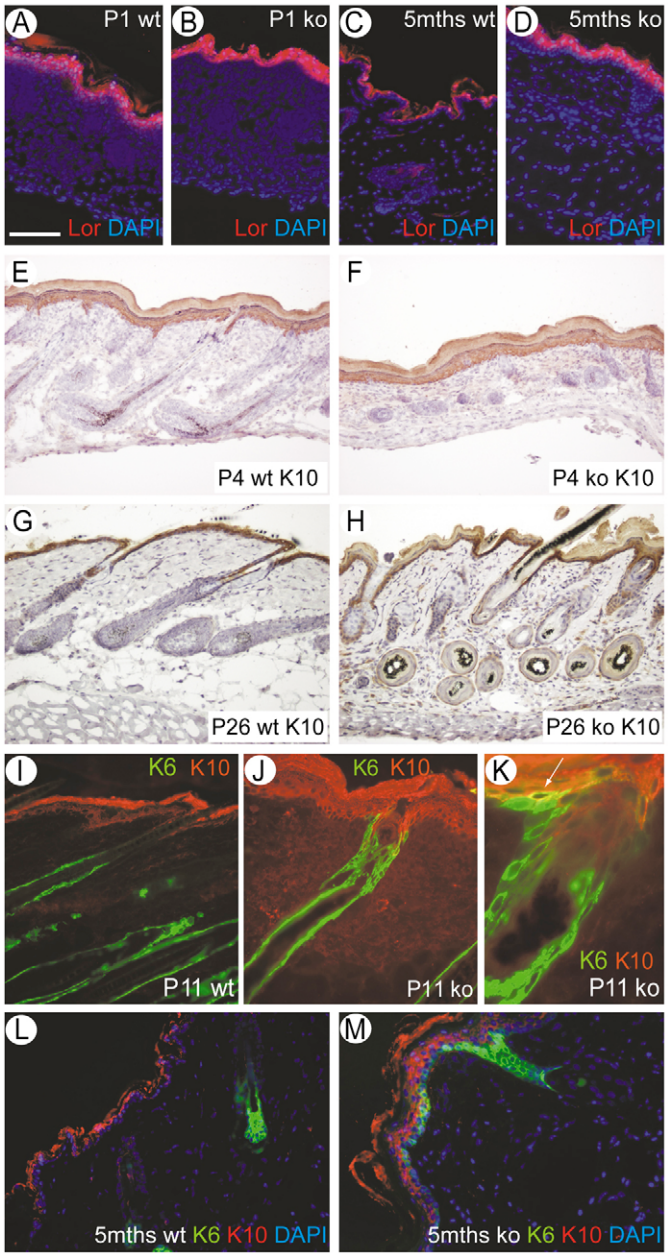

Fig. 7. Skin localization of differentiation and proliferation markers in control and K14-*Gata3*$^{-/-}$ skin. (**A-D**) Normal staining of the late-stage differentiation marker loricrin at P1 (A,B) and 5 months (C,D). (**E**,**F**) Normal staining of the differentiation marker K10 at P4. (**G**,**H**) K10 expression at P26; note the cyst-like HFs in K14-*Gata3*$^{-/-}$. (**I-M**) Double-labelling of K10 (red) and K6 (green) at P11 (I-K) and at 5 months (L,M). There are clearly separated expression domains in the wt (I), but in K14-*Gata3*$^{-/-}$ K6 expression extends more distally (J); the arrow in K indicates a double-labelled (yellow) cell present in the K14-*Gata3*$^{-/-}$. Scale bar in A: 200 μm for A-H; 150 μm for I,J,L,M; 10 μm for K.

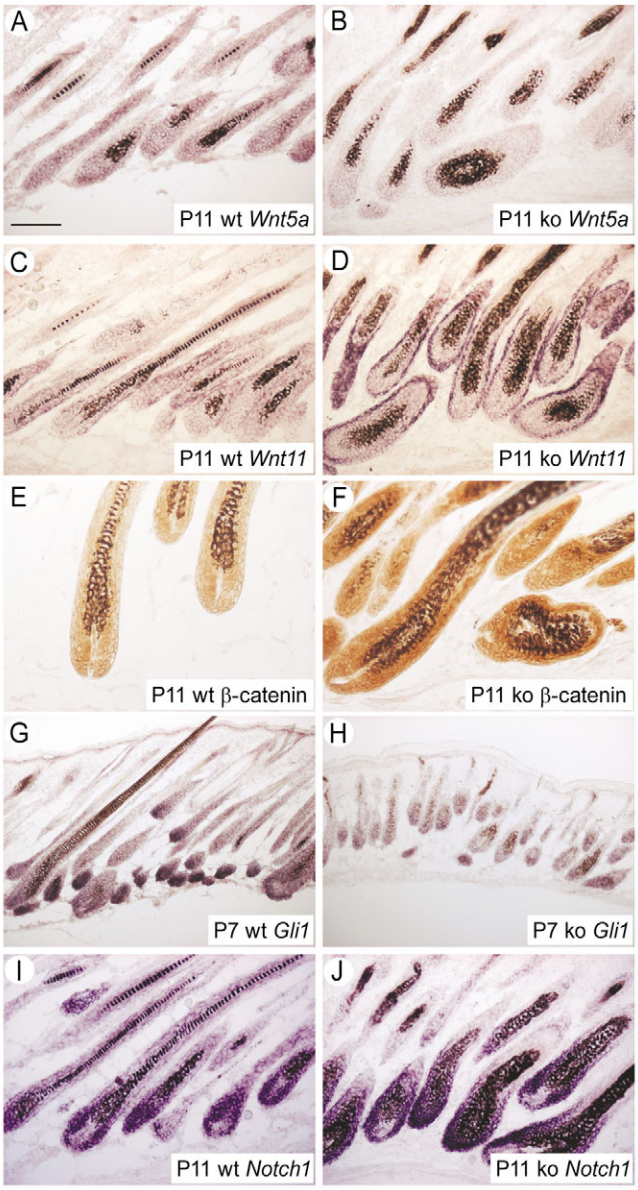

Fig. 8. Expression pattern of signalling molecules in HFs in the absence of Gata3. (**A**,**B**) Reduced expression levels of *Wnt5a* in K14-*Gata3*$^{-/-}$ HFs (B) as compared with wt littermate controls (A). (**C**,**D**) Increased *Wnt11* expression in the K14-*Gata3*$^{-/-}$ outer HF layer (D) as compared with wt controls (C) at P11. (**E**,**F**) Stronger nuclear β-catenin staining in K14-*Gata3*$^{-/-}$ HFs in the matrix and in the distal part of the HF (F) as compared with control (E) at P11. (**G**,**H**) Decrease in *Gli1* expression levels, particularly in the region of the dermal papilla in P7 K14-*Gata3*$^{-/-}$ HFs (H) as compared with controls (G). (**I**,**J**) Higher expression levels of *Notch1* at P11 in the K14-*Gata3*$^{-/-}$ HF (J) as compared with wt (I). Scale bar in A: 150 μm for A-D,I,J; 100 μm for E,F; 200 μm for G,H.

demonstrate significant changes. We examined BMP targets (Smad1/5/8-*P* and Id2) and an antagonist (gremlin) in the K14-*Gata3*$^{-/-}$ in greater detail (see Fig. S5 in the supplementary material). In situ hybridization showed slightly elevated expression of *Bpm6* in K14-*Gata3*$^{-/-}$ HFs compared with controls (see Fig. S5A,B in the supplementary material). Phosphorylation of Smad1/5/8 proteins was higher and more expanded in K14-*Gata3*$^{-/-}$ HFs, especially in the matrix and epidermis (see Fig. S5D,F in the supplementary material). Interestingly, the expression of the BMP antagonist gremlin, which is expressed in the Henle's layer, was absent in K14-Gata3$^{-/-}$ HFs (see Fig. S5G,H in the supplementary material). Id2 protein (a target for BMPs) was expressed in the cuticule of IRS, epidermis and in the distal ORS, but was absent in proximal K14-*Gata3*$^{-/-}$ HF (see Fig. S5I-K in the supplementary material), whereas it was upregulated in epidermis and in the distal part of HF in K14-*Gata3*$^{-/-}$ skin (see Fig. S5L in the supplementary material).

The majority of transcription factors are upregulated in K14-*Gata3*$^{-/-}$ HFs

Several transcription factors demonstrated deviant expression profiles in the K14-*Gata3*$^{-/-}$ HF (see Table S1 in the supplementary material), although differences were smaller than those of structural genes. The majority of transcription factors were overexpressed in the K14-*Gata3*$^{-/-}$ HF (27 up, 12 down) indicating that Gata3 can function as a transcriptional repressor (and activator) in line with recent data showing that Gata factors interact with Fog1 (Zfpm1 – Mouse Genome Informatics) to form repressive chromatin complexes (Rodriguez et al., 2005). *Cutl1*, which encodes the transcriptional repressor CDP known to be involved in epidermal differentiation, was downregulated in the K14-*Gata3*$^{-/-}$ mice (Fig. 4H). However, the hair phenotype of *Cutl1*$^{-/-}$ mice (e.g. circle hairs, corkscrew hairs) as well as several documented transcriptional changes are different to those of K14-*Gata3*$^{-/-}$ mice (Ellis et al., 2001), suggesting that CDP and Gata3 are likely to function in distinct signaling pathways.

Stem cell markers in K14-*Gata3*$^{-/-}$ skin

To analyze the presence and distribution of bulge cells in the K14-*Gata3*$^{-/-}$ skin and to delineate the role of Gata3 in the formation of the bulge, we investigated the expression of stem cell markers keratin 15 and S100A6 (Blanpain et al., 2004; Kizawa and Ito, 2005; Cotsarelis, 2006). Compared to wt skin, keratin 15 and S100A6 were dramatically upregulated in the distal K14-*Gata3*$^{-/-}$ HF and were also present in the epidermis at P11, P19 and 5 months. Whereas the HF and epidermis expression domains are disconnected in wt, they form a continuum in the K14-*Gata3*$^{-/-}$ mice (see Fig. S6 in the supplementary material), suggesting that the bulge contributes more to the knockout epidermis and that Gata3 function is different in the epidermis than in the HF. As a result, the bulge also appears to contribute to epidermal thickening in addition to the increased proliferation of the epidermal cells (Fig. 5A,B). To obtain additional evidence for the contribution of the HF to the epidermis, we examined the bald inside of the ear versus the outside, which does have many HF. Interestingly, K6, the marker for proliferating cells, is absent in epidermis from both the inside and outside of the ear, but is present in HF (Fig. 9A). In K14-*Gata3*$^{-/-}$ the epidermis on the outside of the ear expresses K6, whereas the inside, that never had HFs, remains K6-negative (Fig. 9B).

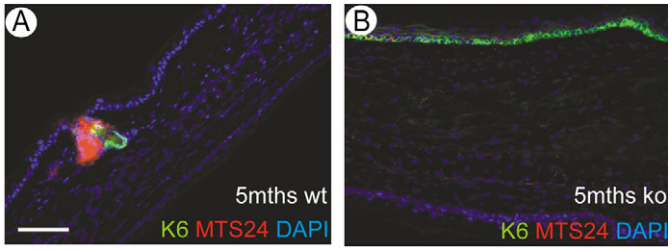

Fig. 9. K6 expression pattern in the ear. Expression of K6 (green) versus MTS24 (red), which marks specific progenitor cells in the HF (Nijhof et al., 2006), at 5 months in wt (A) and K14-*Gata3*$^{-/-}$ (B) ears. The epidermis on the outside of the ear is towards the top of the image; the epidermis on the inside of the ear is towards the bottom of the image. Scale bar: 150 μm.

DISCUSSION

Gata3 is essential for proper maintenance of the epidermis and hair follicle cycling

Deletion of the *Gata3* gene in the murine epidermis and HF results in postnatal growth and developmental abnormalities along with aberrant hair growth, abnormal HF organization and pigmentation and pronounced epidermal thickening. This was followed by the gradual appearance of skin wrinkles, and one layer of the HF, the IRS, was not properly formed (see also Kaufman et al., 2003). In the present study, Gata3 is also expressed in layers other than the IRS of the HF, and all layers are disturbed. Normally, cells in the bulge reform the proximal part of the HF to replace shed hairs by new ones. This process does not take place in the K14-*Gata3*$^{-/-}$ knockout resulting in bald mice. Despite their disoriented appearance, the number of HFs was not substantially reduced, suggesting that Gata3 is not essential for the early steps of HF induction. Instead, Gata3 appears to have a role in hair cycling, as bulge cells no longer give rise to a new follicle. This is consistent with *Gata3*$^{-/-}$ skin grafting experiments showing that, in the absence of Gata3, the hair structures are still apparent in very early skin although with an aberrant morphology. The *Gata3*$^{-/-}$ skin was not analyzed at later stages in those transplantation experiments (Kaufman et al., 2003).

Gata3 impinges on the distribution of proliferating cells in the hair follicle matrix

Despite significant advances in our understanding of the role of Gata3 in HF development, little is known about those biological processes most significantly affected in the absence of Gata3 in the murine epidermis and HFs. We implemented a full mouse transcriptome analysis in laser-captured HFs to get an unbiased insight into: (1) the implicated biological processes; (2) the signalling mechanisms involved; and (3) the nature of the defect itself. This approach revealed several processes most pertinent to the cell cycle, epithelial growth and differentiation and signal transduction pathways. Importantly, we identified a broad, uniform decrease in the expression of most genes associated with the transition of the mitotic cell cycle. However, subsequent evaluation with BrdU staining revealed that, although the overall number of BrdU(+) cells did not differ between the K14-*Gata3*$^{-/-}$ and wt HFs, there was a significant difference in the distribution of proliferating cells throughout the HF. These findings highlight the direct role of Gata3 in differentially regulating specific cell lineages that originate from the matrix area and, together with previous data (Kaufman et al., 2003), suggest that loss of Gata3 negatively impacts on proliferation and cell fate decisions in the matrix, which is likely to

shift matrix cells towards fates other than the inner root sheath. Consistent with the decreased proliferative capacity of those cells located in the basal layer of the HF, apoptosis was reduced in the K14-*Gata3*$^{-/-}$ HF, which is likely to reflect the delayed onset of growth and differentiation. In agreement, several pro-apoptotic genes were downregulated whereas anti-apoptotic genes were upregulated. Coupled to this response, a number of genes involved in histone metabolism and chromatin modification were significantly upregulated in the absence of Gata3 from the HF.

Epithelial growth and differentiation represent significantly affected processes in the K14-*Gata3*$^{-/-}$ HF

Notably, changes in expression of genes encoding keratins and keratin-associated proteins were amongst the broadest identified. IRS cells express a number of genes that are also expressed in the suprabasal epidermal layers, suggesting that both cell types employ comparable differentiation pathways (Botchkarev and Paus, 2003). K10 expression is activated in terminally differentiated epidermal keratinocytes, when they start losing their proliferative competence. Conversely, K10 expression is severely reduced under conditions that promote proliferation (Fuchs and Green, 1980; Fuchs and Weber, 1994; Moll et al., 1982), whereas ectopic K10 expression can induce an Rb-mediated cell cycle arrest (Paramio et al., 1999; Santos et al., 2002). By contrast, K14-*Gata3*$^{-/-}$ mice express (ectopic) K10 in proliferating basal epidermal cells and in the decreased proliferating cells in the bulb of the HF. By analogy to Gata1 (Rodriguez et al., 2005), this suggests that Gata3 has (at least) a dual regulatory function affecting a number of genes involved in cell proliferation and terminal differentiation.

K10 expression is also regulated by the transcription factors C/EBP and AP-2 (Tcfap2a – Mouse Genome Informatics) (Maytin et al., 1999). Despite certain differences between the *Cebpβ*$^{-/-}$ and K14-*Gata3*$^{-/-}$ mice, some phenotypic parallels are striking. Although in *Cebpβ*$^{-/-}$ mice the epidermis, the dermis and the size and number of HFs appear normal, K10 expression is expanded similar to the K14-*Gata3*$^{-/-}$ mice and subcutaneous fat is also decreased (Maytin et al., 1999). Interestingly, the two C/EBP-binding sites in the *K10* (*Krt10* – Mouse Genome Informatics) promoter flank a highly conserved GATA-binding site, suggesting that Gata3 and C/EBP regulate K10.

Wnt and BMP signalling pathways in the K14-*Gata3*$^{-/-}$ hair follicle

Wnt signaling regulates HF development. Mice lacking Lef1, a downstream Wnt mediator, demonstrate a reduced number of body hairs (van Genderen et al., 1994), whereas ectopic expression of either Lef1 or constitutively active β-catenin induces ectopic HFs (Gat et al., 1998; Noramly et al., 1999; Zhou et al., 1995). Upon Wnt signaling, β-catenin accumulates in the cytoplasm and is transported to the nucleus, where it interacts with members of the LEF/TCF family of transcription factors, thereby activating the expression of downstream gene targets (Barker et al., 2000). K14-*Gata3*$^{-/-}$ show a considerable change in Wnt-related protein expression (Fig. 4, Fig. 8E,F), which probably underlies the abnormal hair formation (DasGupta and Fuchs, 1999). Our results are in agreement with those obtained in *Bmpr1a*$^{-/-}$ mice, which have decreased levels of Gata3 (Andl et al., 2004; Ming Kwan, 2004; Yuhki et al., 2004).

Interestingly, all BMP family genes whose expression changes significantly in the K14-*Gata3*$^{-/-}$ mice (*Bmp6*, *Bmp8a* and *Bmp15*) were upregulated (Fig. 5H). Moderately elevated Bmp6 signalling leads to increased proliferation of basal epidermal keratinocytes (Blessing et al., 1996; Botchkarev et al., 1999), similar to that observed in the K14-*Gata3*$^{-/-}$ basal epidermal layer. However, the phenotype of mice overexpressing Bmp6 in the suprabasal epidermis (Blessing et al., 1996) is distinct from that seen in K14-*Gata3*$^{-/-}$ mice.

FGF and Notch1 signalling pathways in the K14-*Gata3*$^{-/-}$ hair follicle

Of all FGF family members (see Table S1 in the supplementary material) only *Fgf5* was downregulated in K14-*Gata3*$^{-/-}$ mice, whereas *Fgfr2* demonstrated increased mRNA expression levels. Mutation of *Fgf5* (Hebert et al., 1994) or expression of a dominant negative *Fgfr2* (Schlake, 2005) leads to the growth of long thin hair, whereas *Fgfr2*$^{-/-}$ mice (Petiot et al., 2003) have a decreased number of HFs, impaired hair formation and reduced basal epidermal cell proliferation. Although, the number of HFs was not affected in K14-*Gata3*$^{-/-}$ mice, *Fgf5* was downregulated, as opposed to increased expression of its receptor, suggesting that the receptor expression is likely to be rate-limiting. Lastly, Notch1 was upregulated in K14-*Gata3*$^{-/-}$ mice. As Notch1 expression, driven by involucrin in the IRS and suprabasal epidermis (Uyttendaele et al., 2004), provokes a similar, yet less severe hair phenotype, our findings highlight the possibility of Notch1 directly affecting hair formation.

In essence, several transgenic and/or knockout mouse models display phenotypic overlap (e.g. epidermal hyperplasia, reduced HF growth). In the majority of these cases, the hair phenotype is frequently accompanied by changes in adipogenesis and fat metabolism, previously thought to be an indirect effect. In addition, increased or reduced expression levels for certain genes, including *Hoxc13* (Godwin and Capecchi, 1998; Tkatchenko et al., 2001), BMP genes (Blessing et al., 1996; Botchkarev et al., 2002) and *Notch1* (Uyttendaele et al., 2004; Vauclair et al., 2005), associated with the signaling mechanisms in hair formation appear to exert similar effects. However, for the majority of genes, it becomes increasingly apparent that their exact temporal and spatial expression is crucial; whereas reduction in *Shh* expression levels results in disturbed HF growth (St-Jacques et al., 1998), its increase leads to epidermal hyper-proliferation with distinct phenotypic features (Ellis et al., 2003).

Our results show that Gata3 is a key transcription factor that impinges on the regulation of several processes resulting in a composite of the phenotypes described above. The changes in keratin expression suggest that Gata3 acts as a moderator between HF development and epidermal differentiation through the orchestrated regulation of distinct signal transduction pathways. If Gata3 levels are greatly diminished, the epidermis hyperproliferates and HF matrix cells do not develop into functional IRS cells. Instead, the HF appears to contribute to the basal epidermis. This switch in mode of action has previously been proposed for Notch1 (Uyttendaele et al., 2004), a negatively regulated target of Gata3. In turn, BMPs regulate Gata3 (Andl et al., 2004; Kobielak et al., 2003) and vice versa (this paper) to maintain appropriate Gata3 expression levels. We therefore propose that Gata3 is a crucial component in the choice between forming different layers of the HF versus basal epidermal cells maintaining their balance through the coordinated regulation of the BMP and Notch signaling pathways.

We are grateful to Jos Jonkers for the K14 cre mice; Wilfred van IJcken and his staff of the Center of Biomics for running the microarrays; Heleen van Beusekom for help with SEM; Leslie van der Fits for inflammation studies; Riccardo Fodde and Patrick Franken for anti-keratin 6 and 14 Abs; T. T. Sun (NY

University School of Medicine) for AE13 and AE15 Abs; Joanne Nijhof for MTS24 Ab; Mark Wijgerde for *Shh* probe; and Katrin Ottersbach for the cyclin D1 probe. This work was supported by the Dutch Organization for Scientific Research (NWO) and by the EU (the NoE CiO).

Supplementary material

Supplementary material for this article is available at http://dev.biologists.org/cgi/content/full/134/2/261/DC1

References

Andl, T., Ahn, K., Kairo, A., Chu, E. Y., Wine-Lee, L., Reddy, S. T., Croft, N. J., Cebra-Thomas, J. A., Metzger, D., Chambon, P. et al. (2004). Epithelial Bmpr1a regulates differentiation and proliferation in postnatal hair follicles and is essential for tooth development. *Development* **131**, 2257-2268.

Aoki, N., Ito, K. and Ito, M. (2000). mu-Crystallin, thyroid hormone-binding protein, is expressed abundantly in the murine inner root sheath cells. *J. Invest. Dermatol.* **115**, 402-405.

Barker, N., Morin, P. J. and Clevers, H. (2000). The Yin-Yang of TCF/beta-catenin signaling. *Adv. Cancer Res.* **77**, 1-24.

Blanpain, C., Lowry, W. E., Geoghegan, A., Polak, L. and Fuchs, E. (2004). Self-renewal, multipotency, and the existence of two cell populations within an epithelial stem cell niche. *Cell* **118**, 635-648.

Blessing, M., Schirmacher, P. and Kaiser, S. (1996). Overexpression of bone morphogenetic protein-6 (BMP-6) in the epidermis of transgenic mice: inhibition or stimulation of proliferation depending on the pattern of transgene expression and formation of psoriatic lesions. *J. Cell Biol.* **135**, 227-239.

Botchkarev, V. A. and Paus, R. (2003). Molecular biology of hair morphogenesis: development and cycling. *J. Exp. Zoolog. Part B Mol. Dev. Evol.* **298**, 164-180.

Botchkarev, V. A., Botchkareva, N. V., Roth, W., Nakamura, M., Chen, L. H., Herzog, W., Lindner, G., McMahon, J. A., Peters, C., Lauster, R. et al. (1999). Noggin is a mesenchymally derived stimulator of hair-follicle induction. *Nat. Cell Biol.* **1**, 158-164.

Botchkarev, V. A., Botchkareva, N. V., Sharov, A. A., Funa, K., Huber, O. and Gilchrest, B. A. (2002). Modulation of BMP signaling by noggin is required for induction of the secondary (nontylotrich) hair follicles. *J. Invest. Dermatol.* **118**, 3-10.

Buchholz, F., Angrand, P. O. and Stewart, A. F. (1998). Improved properties of FLP recombinase evolved by cycling mutagenesis. *Nat. Biotechnol.* **16**, 657-662.

Cotsarelis, G. (2006). Epithelial stem cells: a folliculocentric view. *J. Invest. Dermatol.* **126**, 1459-1468.

Cotsarelis, G., Sun, T. T. and Lavker, R. M. (1990). Label-retaining cells reside in the bulge area of pilosebaceous unit: implications for follicular stem cells, hair cycle, and skin carcinogenesis. *Cell* **61**, 1329-1337.

DasGupta, R. and Fuchs, E. (1999). Multiple roles for activated LEF/TCF transcription complexes during hair follicle development and differentiation. *Development* **126**, 4557-4568.

Ellis, T., Gambardella, L., Horcher, M., Tschanz, S., Capol, J., Bertram, P., Jochum, W., Barrandon, Y. and Busslinger, M. (2001). The transcriptional repressor CDP (Cutl1) is essential for epithelial cell differentiation of the lung and the hair follicle. *Genes Dev.* **15**, 2307-2319.

Ellis, T., Smyth, I., Riley, E., Bowles, J., Adolphe, C., Rothnagel, J. A., Wicking, C. and Wainwright, B. J. (2003). Overexpression of Sonic Hedgehog suppresses embryonic hair follicle morphogenesis. *Dev. Biol.* **263**, 203-215.

Fuchs, E. and Green, H. (1980). Changes in keratin gene expression during terminal differentiation of the keratinocyte. *Cell* **19**, 1033-1042.

Fuchs, E. and Weber, K. (1994). Intermediate filaments: structure, dynamics, function, and disease. *Annu. Rev. Biochem.* **63**, 345-382.

Fuchs, E., Tumbar, T. and Guasch, G. (2004). Socializing with the neighbors: stem cells and their niche. *Cell* **116**, 769-778.

Gat, U., DasGupta, R., Degenstein, L. and Fuchs, E. (1998). De Novo hair follicle morphogenesis and hair tumors in mice expressing a truncated beta-catenin in skin. *Cell* **95**, 605-614.

Gill, J., Malin, M., Hollander, G. A. and Boyd, R. (2002). Generation of a complete thymic microenvironment by MTS24(+) thymic epithelial cells. *Nat. Immunol.* **3**, 635-642.

Godwin, A. R. and Capecchi, M. R. (1998). Hoxc13 mutant mice lack external hair. *Genes Dev.* **12**, 11-20.

Hardman, M. J., Sisi, P., Banbury, D. N. and Byrne, C. (1998). Patterned acquisition of skin barrier function during development. *Development* **125**, 1541-1552.

Hardy, M. H. (1992). The secret life of the hair follicle. *Trends Genet* **8**, 55-61.

Hebert, J. M., Rosenquist, T., Gotz, J. and Martin, G. R. (1994). FGF5 as a regulator of the hair growth cycle: evidence from targeted and spontaneous mutations. *Cell* **78**, 1017-1025.

Hosack, D. A., Dennis, G., Jr, Sherman, B. T., Lane, H. C. and Lempicki, R. A. (2003). Identifying biological themes within lists of genes with EASE. *Genome Biol.* **4**, R70.

Jonkers, J., Meuwissen, R., van der Gulden, H., Peterse, H., van der Valk, M. and Berns, A. (2001). Synergistic tumor suppressor activity of BRCA2 and p53 in a conditional mouse model for breast cancer. *Nat. Genet.* **29**, 418-425.

Kaufman, C. K., Zhou, P., Pasolli, H. A., Rendl, M., Bolotin, D., Lim, K. C., Dai, X., Alegre, M. L. and Fuchs, E. (2003). GATA-3: an unexpected regulator of cell lineage determination in skin. *Genes Dev.* **17**, 2108-2122.

Kizawa, K. and Ito, M. (2005). Characterization of epithelial cells in the hair follicle with S100 proteins. *Methods Mol. Biol.* **289**, 209-222.

Kobielak, K., Pasolli, H. A., Alonso, L., Polak, L. and Fuchs, E. (2003). Defining BMP functions in the hair follicle by conditional ablation of BMP receptor IA. *J. Cell Biol.* **163**, 609-623.

Kopan, R. and Weintraub, H. (1993). Mouse notch: expression in hair follicles correlates with cell fate determination. *J. Cell Biol.* **121**, 631-641.

Legue, E. and Nicolas, J. F. (2005). Hair follicle renewal: organization of stem cells in the matrix and the role of stereotyped lineages and behaviors. *Development* **132**, 4143-4154.

Lynch, M. H., O'Guin, W. M., Hardy, C., Mak, L. and Sun, T. T. (1986). Acidic and basic hair/nail ("hard") keratins: their colocalization in upper cortical and cuticle cells of the human hair follicle and their relationship to "soft" keratins. *J. Cell Biol.* **103**, 2593-2606.

Maytin, E. V., Lin, J. C., Krishnamurthy, R., Batchvarova, N., Ron, D., Mitchell, P. J. and Habener, J. F. (1999). Keratin 10 gene expression during differentiation of mouse epidermis requires transcription factors C/EBP and AP-2. *Dev. Biol.* **216**, 164-181.

Ming Kwan, K., Li, A. G., Wang, X.-J., Wurst, W. and Behringer, R. R. (2004). Essential roles of BMPR-IA signaling in differentiation and growth of hair follicles and in skin tumorigenesis. *Genesis* **39**, 10-25.

Moll, R., Franke, W. W., Schiller, D. L., Geiger, B. and Krepler, R. (1982). The catalog of human cytokeratins: patterns of expression in normal epithelia, tumors and cultured cells. *Cell* **31**, 11-24.

Morris, R. J., Liu, Y., Marles, L., Yang, Z., Trempus, C., Li, S., Lin, J. S., Sawicki, J. A. and Cotsarelis, G. (2004). Capturing and profiling adult hair follicle stem cells. *Nat. Biotechnol.* **22**, 411-417.

Nijhof, J. G., Braun, K. M., Giangreco, A., van Pelt, C., Kawamoto, H., Boyd, R. L., Willemze, R., Mullenders, L. H., Watt, F. M., de Gruijl, F. R. et al. (2006). The cell-surface marker MTS24 identifies a novel population of follicular keratinocytes with characteristics of progenitor cells. *Development* **133**, 3027-3037.

Noramly, S., Freeman, A. and Morgan, B. A. (1999). beta-catenin signaling can initiate feather bud development. *Development* **126**, 3509-3521.

O'Guin, W. M., Sun, T. T. and Manabe, M. (1992). Interaction of trichohyalin with intermediate filaments: three immunologically defined stages of trichohyalin maturation. *J. Invest. Dermatol.* **98**, 24-32.

Oliver, R. F. and Jahoda, C. A. (1988). Dermal-epidermal interactions. *Clin. Dermatol.* **6**, 74-82.

Oshima, H., Rochat, A., Kedzia, C., Kobayashi, K. and Barrandon, Y. (2001). Morphogenesis and renewal of hair follicles from adult multipotent stem cells. *Cell* **104**, 233-245.

Pandolfi, P. P., Roth, M. E., Karis, A., Leonard, M. W., Dzierzak, E., Grosveld, F. G., Engel, J. D. and Lindenbaum, M. H. (1995). Targeted disruption of the GATA3 gene causes severe abnormalities in the nervous system and in fetal liver haematopoiesis. *Nat. Genet.* **11**, 40-44.

Paramio, J. M., Casanova, M. L., Segrelles, C., Mittnacht, S., Lane, E. B. and Jorcano, J. L. (1999). Modulation of cell proliferation by cytokeratins K10 and K16. *Mol. Cell. Biol.* **19**, 3086-3094.

Pata, I., Studer, M., van Doorninck, J. H., Briscoe, J., Kuuse, S., Engel, J. D., Grosveld, F. and Karis, A. (1999). The transcription factor GATA3 is a downstream effector of Hoxb1 specification in rhombomere 4. *Development* **126**, 5523-5531.

Petiot, A., Conti, F. J., Grose, R., Revest, J. M., Hodivala-Dilke, K. M. and Dickson, C. (2003). A crucial role for Fgfr2-IIIb signalling in epidermal development and hair follicle patterning. *Development* **130**, 5493-5501.

Reddy, S., Andl, T., Bagasra, A., Lu, M. M., Epstein, D. J., Morrisey, E. E. and Millar, S. E. (2001). Characterization of Wnt gene expression in developing and postnatal hair follicles and identification of Wnt5a as a target of Sonic hedgehog in hair follicle morphogenesis. *Mech. Dev.* **107**, 69-82.

Rodriguez, P., Bonte, E., Krijgsveld, J., Kolodziej, K. E., Guyot, B., Heck, A. J., Vyas, P., de Boer, E., Grosveld, F. and Strouboulis, J. (2005). GATA-1 forms distinct activating and repressive complexes in erythroid cells. *EMBO J.* **24**, 2354-2366.

Santos, M., Paramio, J. M., Bravo, A., Ramirez, A. and Jorcano, J. L. (2002). The expression of keratin k10 in the basal layer of the epidermis inhibits cell proliferation and prevents skin tumorigenesis. *J. Biol. Chem.* **277**, 19122-19130.

Schaeren-Wiemers, N. and Gerfin-Moser, A. (1993). A single protocol to detect transcripts of various types and expression levels in neural tissue and cultured cells: in situ hybridization using digoxigenin-labelled cRNA probes. *Histochemistry* **100**, 431-440.

Schlake, T. (2005). FGF signals specifically regulate the structure of hair shaft medulla via IGF-binding protein 5. *Development* **132**, 2981-2990.

Schmidt-Ullrich, R. and Paus, R. (2005). Molecular principles of hair follicle induction and morphogenesis. *BioEssays* **27**, 247-261.

St-Jacques, B., Dassule, H. R., Karavanova, I., Botchkarev, V. A., Li, J., Danielian, P. S., McMahon, J. A., Lewis, P. M., Paus, R. and McMahon, A. P. (1998). Sonic hedgehog signaling is essential for hair development. *Curr. Biol.* **8**, 1058-1068.

Taylor, G., Lehrer, M. S., Jensen, P. J., Sun, T. T. and Lavker, R. M. (2000). Involvement of follicular stem cells in forming not only the follicle but also the epidermis. *Cell* **102**, 451-461.

Tkatchenko, A. V., Visconti, R. P., Shang, L., Papenbrock, T., Pruett, N. D., Ito, T., Ogawa, M. and Awgulewitsch, A. (2001). Overexpression of Hoxc13 in differentiating keratinocytes results in downregulation of a novel hair keratin gene cluster and alopecia. *Development* **128**, 1547-1558.

Uyttendaele, H., Panteleyev, A. A., de Berker, D., Tobin, D. T. and Christiano, A. M. (2004). Activation of Notch1 in the hair follicle leads to cell-fate switch and Mohawk alopecia. *Differentiation* **72**, 396-409.

van Genderen, C., Okamura, R. M., Farinas, I., Quo, R. G., Parslow, T. G., Bruhn, L. and Grosschedl, R. (1994). Development of several organs that require inductive epithelial-mesenchymal interactions is impaired in LEF-1-deficient mice. *Genes Dev.* **8**, 2691-2703.

Vassar, R., Rosenberg, M., Ross, S., Tyner, A. and Fuchs, E. (1989). Tissue-specific and differentiation-specific expression of a human K14 keratin gene in transgenic mice. *Proc. Natl. Acad. Sci. USA* **86**, 1563-1567.

Vassar, R., Coulombe, P. A., Degenstein, L., Albers, K. and Fuchs, E. (1991). Mutant keratin expression in transgenic mice causes marked abnormalities resembling a human genetic skin disease. *Cell* **64**, 365-380.

Vauclair, S., Nicolas, M., Barrandon, Y. and Radtke, F. (2005). Notch1 is essential for postnatal hair follicle development and homeostasis. *Dev. Biol.* **284**, 184-193.

Yuhki, M., Yamada, M., Kawano, M., Iwasato, T., Itohara, S., Yoshida, H., Ogawa, M. and Mishina, Y. (2004). BMPR1A signaling is necessary for hair follicle cycling and hair shaft differentiation in mice. *Development* **131**, 1825-1833.

Zhou, P., Byrne, C., Jacobs, J. and Fuchs, E. (1995). Lymphoid enhancer factor 1 directs hair follicle patterning and epithelial cell fate. *Genes Dev.* **9**, 700-713.